Theoretical study of the C^- $^4S^o_{3/2}$ and $^2D^o_{3/2,5/2}$ bound states and C ground configuration: Fine and hyperfine structures, isotope shifts, and transition probabilities

T. Carette* and M. R. Godefroid†

Chimie quantique et photophysique, CP160/09, Université Libre de Bruxelles, B-1050 Brussels, Belgium

(Received 27 January 2011; published 8 June 2011)

This work is an *ab initio* study of the $2p^3\ ^4S^o_{3/2}$, and $^2D^o_{3/2,5/2}$ states of C^- and $2p^2\ ^3P_{0,1,2}$, $^1D_2$, and $^1S_0$ states of neutral carbon. We use the multiconfiguration Hartree-Fock approach, focusing on the accuracy of the wave function itself. We obtain all C^- detachment thresholds, including correlation effects to about 0.5%. Isotope shifts and hyperfine structures are calculated. The achieved accuracy of the latter is of the order of 0.1 MHz. Intraconfiguration transition probabilities are also estimated.

DOI: 10.1103/PhysRevA.83.062505 PACS number(s): 32.10.Hq, 31.15.ac, 31.15.ag, 32.10.Fn

I. INTRODUCTION

Negative ions have always attracted broad attention from the scientific community [1,2]. They challenge both the experimentalists and theoreticians; the first because they are weakly bound, and therefore fragile, and because they do not possess many features allowing measurements, and the latter because the binding of an extra electron is granted only by an arrangement of the electrons in a highly correlated system [3]. Moreover, the fact that the electrons in negative ions are bound by a short-range potential confer them unique properties.

C^- is the lightest negative ion to have two bound terms: its ground state $^4S^o$ and the $^2D^o$ excited state which both arise from the $2p^3$ configuration. The level diagram of the states studied in this work is given in Fig. 1.

Carbon is among the most abundant components in the universe and a key element in life chemistry. The carbon negative ion is important in astrophysics and atmosphere physics since nitrogen-like $2p^3\ ^4S^o$-$^2D^o$ forbidden lines are recognized as useful transitions for abundances determination [4–6]. It has also recently been suggested by Le Padellec *et al.* [7] that C^- negative ion could intervene in astrophysical reactions. The photodetachment cross-sections of the C^- have been repeatedly studied, both theoretically [8] and experimentally [9], for photon energies addressing valence electrons and core electrons [10,11]. Recently, an isotope separation method was tested by Andersson *et al.* [12], based on the isotopic dependence of the Doppler shift of the C^- detachment thresholds in an accelerator.

A binding energy of 1.262119(20) eV for the $C^-(^4S^o)$ has been measured by Scheer *et al.* [13], who could not improve the old value of 33(1) meV for the $C^-(^2D^o)$ detachment threshold, measured by Feldmann [14]. The fine structure of the $^2D^o$ state is not known. On the theoretical side, very accurate carbon electron affinities were obtained with coupled-cluster-based methods [15–17].

The structure of the C^- has not been studied thoroughly and especially little is known about the $^2D^o$ multiplet. In laboratory plasmas, lifetimes of the order of the ms were measured for the $C^-(^2D^o)$, the electron detachment being principally caused by the black-body radiation and, to a lesser extent, to collisions [18]. Significantly longer lifetimes could be reached in the cold and diluted interstellar media where molecular anions have already been detected [19]. However, the $C^-(^2D^o)$ is, for various reasons, very difficult to study experimentally. In this context, a firm theoretical knowledge of this system is particularly precious.

Elements from boron to fluorine are the next targets after beryllium in the working line of "exact" calculations. High accuracy can be achieved for systems with up to four electrons using wave functions expanded in explicitly correlated Gaussian or in Hylleraas coordinates [20–22]. Although the precision that can be achieved for atoms with more electrons is limited by the complexity of the electron-correlation mathematical treatment, the ground states of the second period p-block atoms from B to F are satisfactorily described by a nonrelativistic approach on top of which relativistic corrections are added.

A critical benchmark quantity for highly correlated models is the isotope shift (IS) on the electron affinity (^eA) that is doubly sensitive to correlation effects: through the negative ion structure and through the specific mass shift parameter. The multiconfiguration Hartree-Fock method has been successfully used for calculating the IS on the ^eA of O [23], S [24], and Cl [25].

The purpose of the present work is double. Our principal objective is to obtain the crucial informations about the C^- electronic structure for stimulating experimental research on the $^2D^o$ state. Therefore, we focus on quantities that are especially difficult for experimentalists to measure: isotope shifts, hyperfine structures, and transition probabilities. As for the energy separations themselves, we do not try to compete with either the observation or the previous coupled-cluster calculations. We instead use these reliable reference data for assessing the quality of our computational procedure.

Our second objective is to obtain nonrelativistic (NR) wave functions as accurate as possible using the standard tools of the ATSP2K package [26]. For getting the best estimation of the accuracy, we choose to use the same systematical construction of our C and C^- models, avoiding any arbitrary compensation of the "additional" electron correlation of the negative ion compared to the neutral atom.

In Sec. II, we present large-scale numerical multiconfiguration Hartree-Fock (MCHF) calculations (Sec. II E) and relativistic calculations, using the Breit-Pauli (BPCI) approach

*tcarette@ulb.ac.be
†mrgodef@ulb.ac.be

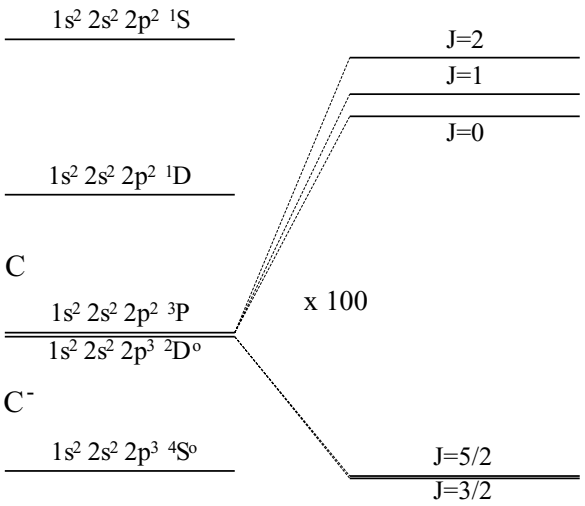

FIG. 1. Levels diagram of C and C^-. The fine structures of C ^3P and C^- $^2D^o$ terms are magnified (×100).

(Sec. II F) [27] and the relativistic configuration (RCI) method based on the Pauli approximation (Sec. II G) [28]. In Sec. III, we present accurate results for hyperfine structures (Sec. III A), total energies including the fine structures (Sec. III B), and mass polarization shift parameters (Sec. III C) of C $2p^2\ ^3P$, ^1D, ^1S and C^- $2p^3\ ^4S^o$, $^2D^o$. In Sec. III D, we present the $M1$ and $E2$ transition probabilities within the $2p^2$ and $2p^3$ configurations of C and C^-.

II. COMPUTATIONAL METHOD

A. The MCHF expansion

The multiconfiguration Hartree-Fock (MCHF) variational approach consists in optimizing the one-electron functions spanning a configuration space and the mixing coefficients of the interacting configuration state functions (CSF) [27] for describing a given term

$$\Psi(\gamma LSM_LM_S) = \sum_i c_i \Phi(\gamma_i LSM_LM_S). \tag{1}$$

B. Hyperfine interaction

The level hyperfine structure is caused by the interaction of the angular momentum of the electrons (**J**) and of the nucleus (**I**), forming the total atomic angular momentum $\mathbf{F} = \mathbf{I} + \mathbf{J}$. The theory underlying the computation of hyperfine structure using MCHF wave functions can be found in Refs. [29–31]. It is possible to express the nonrelativistic hyperfine interaction in terms of the J-independent orbital (a_l), spin-dipole ($a_{\rm sd}$), contact (a_c), and electric quadrupole (b_q) electronic hyperfine parameters defined as [29]

$$a_l \equiv \langle \Gamma LSM_LM_S| \sum_{i=1}^{N} l_0^{(1)}(i) r_i^{-3} |\Gamma LSM_LM_S\rangle, \tag{2}$$

$$a_{\rm sd} \equiv \langle \Gamma LSM_LM_S| \sum_{i=1}^{N} 2C_0^{(2)}(i) s_0^{(1)}(i) r_i^{-3} |\Gamma LSM_LM_S\rangle, \tag{3}$$

$$a_c \equiv \langle \Gamma LSM_LM_S| \sum_{i=1}^{N} 2s_0^{(1)}(i) r_i^{-2} \delta(r_i) |\Gamma LSM_LM_S\rangle, \tag{4}$$

$$b_q \equiv \langle \Gamma LSM_LM_S| \sum_{i=1}^{N} 2C_0^{(2)}(i) r_i^{-3} |\Gamma LSM_LM_S\rangle, \tag{5}$$

and calculated for the magnetic component $M_L = L$ and $M_S = S$ [32]. The diagonal hyperfine interaction energy correction is usually expressed in terms of the hyperfine magnetic dipole (A_J) and electric quadrupole (B_J) constants as follows:

$$W(J,J) = A_J \frac{C}{2} + B_J \frac{3C(C+1) - 4I(I+1)J(J+1)}{8I(2I-1)J(2J-1)}. \tag{6}$$

The first three parameters (2), (3), and (4) contribute to the magnetic dipole hyperfine interaction constant through

$$A_J = A_J^l + A_J^{\rm sd} + A_J^c, \tag{7}$$

with [33]

$$A_J^l = G_\mu \frac{\mu_I}{I}\, a_l\, \frac{\langle \boldsymbol{L}\cdot\boldsymbol{J}\rangle}{LJ(J+1)}, \tag{8}$$

$$A_J^{\rm sd} = \frac{1}{2} G_\mu g_s \frac{\mu_I}{I} a_{\rm sd} \times \frac{3\langle \boldsymbol{L}\cdot\boldsymbol{S}\rangle\langle \boldsymbol{L}\cdot\boldsymbol{J}\rangle - L(L+1)\langle \boldsymbol{S}\cdot\boldsymbol{J}\rangle}{SL(2L-1)J(J+1)}, \tag{9}$$

$$A_J^c = \frac{1}{6} G_\mu g_s \frac{\mu_I}{I} a_c \frac{\langle \boldsymbol{S}\cdot\boldsymbol{J}\rangle}{SJ(J+1)}, \tag{10}$$

while the last one (b_q) constitutes the electronic contribution to the electric quadrupole hyperfine interaction

$$B_J = -\, G_q Q b_q \times \frac{6\langle \boldsymbol{L}\cdot\boldsymbol{J}\rangle^2 - 3\langle \boldsymbol{L}\cdot\boldsymbol{J}\rangle - 2L(L+1)J(J+1)}{L(2L-1)(J+1)(2J+3)}. \tag{11}$$

Expressing the electronic parameters a_l, $a_{\rm sd}$, and a_c in atomic units (units of a_0^{-3}) and μ_I in nuclear magnetons (units of μ_N), the magnetic dipole hyperfine structure constants A_J are calculated in units of frequency (MHz) by using $G_\mu = 95.41067$. Similarly, the electric quadrupole hyperfine structure constants B_J are expressed in MHz when adopting atomic units (units of a_0^{-3}) for b_q, barns for Q and $G_q = 234.96475$. The expectation values of the angular momenta scalar products are given by

$$\langle \boldsymbol{L}\cdot\boldsymbol{J}\rangle = [J(J+1) + L(L+1) - S(S+1)]/2, \tag{12}$$

$$\langle \boldsymbol{S}\cdot\boldsymbol{J}\rangle = [J(J+1) - L(L+1) + S(S+1)]/2, \tag{13}$$

$$\langle \boldsymbol{S}\cdot\boldsymbol{L}\rangle = [J(J+1) - L(L+1) - S(S+1)]/2, \tag{14}$$

when calculated with nonrelativistic LSJ wave functions. The expression for the off-diagonal hyperfine interaction, depending on the hyperfine constants $A_{J,J-1}$, $B_{J,J-1}$, and $B_{J,J-2}$, are developed in Ref. [31]. Hibbert [32] gives the expressions of $A_{J,J-1}$ in terms of the hyperfine parameters (2)–(5).

C. The isotope shift

The first-order isotope shift on an energy level is decomposed in a field shift (or volume shift) and a mass shift [34].

The first is proportional to the change in nucleus rms radius and change of the modified electron density at the origin. It is negligible in our context.

The energy corrected for the first-order mass shift, on the other hand, can be estimated using [35]

$$E_M = \frac{M}{m+M} E_\infty + \frac{Mm}{(M+m)^2} \frac{\hbar^2}{m} S_{\rm sms}, \tag{15}$$

where m is the electron mass, M is the bare nucleus mass, E_∞ the infinite mass nucleus, and

$$S_{\rm sms} = -\langle \Psi_\infty | \sum_{i<j} \nabla_i \cdot \nabla_j | \Psi_\infty \rangle. \tag{16}$$

The first term contains the normal mass shift (NMS)

$$\Delta E_{\rm NMS} = -\frac{m}{m+M} E_\infty \tag{17}$$

and the second one is the specific mass shift (SMS). The mass polarization parameter, $S_{\rm sms}$, has the dimension of an inverse square length.

D. Transition probabilities

The Einstein A_{if} coefficient of spontaneous emission is defined as the total probability per unit of time for an atom in a given energy level i to make a radiative transition to any of the g_f states of the energy level f [36].

A transition between levels of same parity is forbidden in the electric dipole approximation, being in general many orders of magnitude lower than an allowed transition. Two interactions of the same order of magnitude can contribute to the appearance of such transitions: the magnetic dipole and the electric quadrupole radiation-matter interactions. At the nonrelativistic level, a dipole magnetic transition ($M1$) is governed by the electronic magnetic dipole operator that is

$$A^{M1} \propto (E_i - E_f)^3 |\langle \Gamma_f J_f || \boldsymbol{L} + g_s \boldsymbol{S} || \Gamma_i J_i \rangle|^2. \tag{18}$$

In the monoconfiguration approximation, the above matrix element is nonzero only between states of the same configuration and LS. This selection rule is relaxed by configuration and LS mixings, the remaining constraints being that $J_f = J_i, J_i \pm 1$ and that Ψ_i and Ψ_f have the same parity. For its part, an electric quadrupole ($E2$) transition rate is proportional to the electric quadrupole moment matrix element

$$A^{E2} \propto (E_i - E_f)^5 |\langle \Gamma_f J_f || \sum_k r_k^2 C^{(2)}(k) || \Gamma_i J_i \rangle|^2, \tag{19}$$

the sum running on all spatial electron coordinates k. Neglecting the LS term mixing, a necessary condition for A_{E2} to be nonzero is that $S_f - S_i = 0$, $|L_f - L_i| \leqslant 2$, $|L_f + L_i| \geqslant 2$ and that the atomic parity is conserved.

E. Nonrelativistic calculations

We first select a zero-order set of CSFs, the multireference (MR). For all studied states it is the set of single and double excitations of the main configuration to the $n = 2,3$ shells. All the CSFs interacting to first order with the MR are selected and we choose the reverse order for the subshell coupling [24]. The orbital active set is defined as the set of all orbitals characterized by quantum numbers $n \leqslant n_{\rm max}$ and $l \leqslant l_{\rm max}$, and is denoted $\lceil n_{\rm max} l_{\rm max} \rceil$. We perform MCHF calculations defined in the spaces $\lceil 4f \rceil$ to $\lceil 12k \rceil$, denoted MR-I$\lceil n_{\rm max} l_{\rm max} \rceil$.

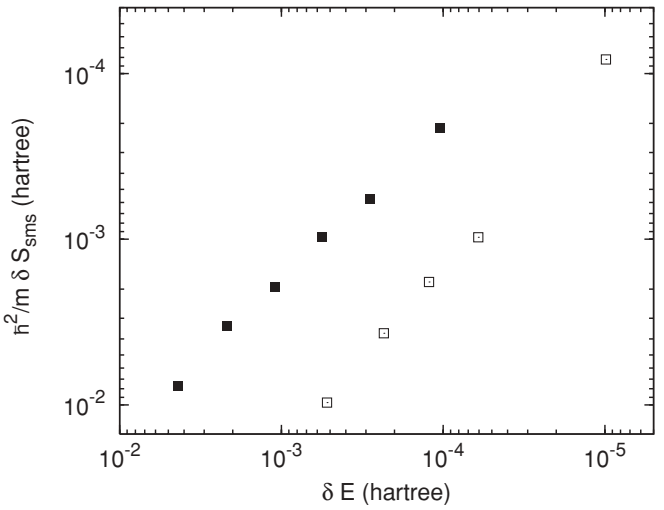

FIG. 2. Bilogarithmic plot of the convergence of the $C(^3P)$ mass polarization expectation value versus the corresponding energy in hartrees. The coordinates of the black squares are the differences (in absolute value) between the results of the MR-I$\lceil nl \rceil$ and MR-I$\lceil 12k \rceil$ calculations, $n = 6$–11 from left to right. Similarly, the coordinates of the white squares show the convergence of MR_p-I$\lceil 12k \rceil$ toward $MR_{99.95}$-I$\lceil 12k \rceil$, $p = (99$–$99.9)\%$ from left to right.

For each active space $\lceil 10k \rceil$, $\lceil 11k \rceil$, and $\lceil 12k \rceil$, we order the configurations according to their weight.[1] We then construct several new MRs following this hierarchy, independently for each state and active set, by selecting the minimum group of configurations that add up to a certain percentage p of the total wave function. Those multireferences are denoted MR_p for each given MR-I wave function. Unsurprisingly, the MR_p sets are not sensitive to the used active set.

Configuration-interaction calculations (CI) that determine the optimal mixing coefficients for a given orbital basis are performed on each MR_p-I CSF sets, p being limited to 99.8% for $C^-(^4S^o)$ and to 99.3% for $C^-(^2D^o)$. An example of the convergence of the calculations with the number of correlation layers $(n-2)$ and p is given in Fig. 2. It presents results on the $2p^2\,{}^3P$ state of neutral carbon. The black squares show $\frac{\hbar^2}{m}\delta S_{\rm sms}$ with

$$\delta S_{\rm sms} = |S_{\rm sms}(\text{MR-I}\lceil nl \rceil) - S_{\rm sms}(\text{MR-I}\lceil 12k \rceil)|, \tag{20}$$

versus

$$\delta E = |E(\text{MR-I}\lceil nl \rceil) - E(\text{MR-I}\lceil 12k \rceil)| \tag{21}$$

for $n = 6$–11. Similarly, the white squares compare the E and $S_{\rm sms}$ convergences of the MR_p-I$\lceil 12k \rceil$, $p = 99.0$–99.9, results toward the $MR_{99.95}$-I$\lceil 12k \rceil$ model. The energy always decreases along a sequence of increasingly large calculations, according to the variational principle, while the $S_{\rm sms}$ of MR_p-I$\lceil nl \rceil$ calculations decreases with n and increases with p. $\delta S_{\rm sms}$ and δE show a close to linear correlation, i.e., the

[1]The weight of a configuration is defined as $w = (\sum_i c_i^2)^{1/2}$, where the sum runs over the CSFs belonging to the configuration.

TABLE I. Results of the MCHF and CI calculations performed for the carbon $2p^2\ ^3P$, ^1D and ^1S terms. The energies E are in units of E_h, the $S_{\rm sms}$ in units of a_0^{-2} and the hyperfine parameters in units of a_0^{-3}. The final values are the results of the larger $\lceil 12k \rceil$ calculations on which the impact of the 13th shell and $l = 8$ orbitals has been additively transferred.

Model		$1s^2 2s^2 2p^2\ ^3P$						$1s^2 2s^2 2p^2\ ^1D$				$1s^2 2s^2 2p^2\ ^1S$	
nl	p	E	$S_{\rm sms}$	a_l	$a_{\rm sd}$	a_c	b_q	E	$S_{\rm sms}$	a_l	b_q	E	$S_{\rm sms}$
				MCHF						MCHF			MCHF
HF		−37.688618	−1.39418	1.69181	0.33836	0.0	0.67672	−37.631331	−1.35557	3.26420	−1.30568	−37.549610	−1.29745
4		−37.823094	−0.43410	1.68577	0.37538	0.26753	0.60177	−37.773728	−0.40151	3.23862	−1.14955	−37.720089	−0.38101
5		−37.834178	−0.40791	1.70216	0.36515	0.59931	0.61023	−37.786495	−0.37677	3.27425	−1.16232	−37.733658	−0.38198
6		−37.839793	−0.39926	1.70450	0.35943	0.46199	0.63127	−37.792593	−0.36238	3.27661	−1.20179	−37.740170	−0.35936
7		−37.842009	−0.40361	1.70480	0.36087	0.42598	0.63566	−37.795060	−0.36697	3.27734	−1.21478	−37.742742	−0.36255
8k		−37.843075	−0.40499	1.70463	0.36235	0.44763	0.63110	−37.796285	−0.36842	3.27694	−1.20731	−37.743993	−0.36275
9k		−37.843607	−0.40598	1.70460	0.36107	0.48183	0.63025	−37.796884	−0.36938	3.27673	−1.20173	−37.744656	−0.36358
10k		−37.843885	−0.40637	1.70460	0.36122	0.46815	0.63195	−37.797231	−0.36991	3.27669	−1.20672	−37.745021	−0.36384
11k		−37.844065	−0.40673	1.70461	0.36136	0.47197	0.63174	−37.797436	−0.37029	3.27665	−1.20611	−37.745234	−0.36417
12k		−37.844170	−0.40695	1.70462	0.36137	0.47401	0.63133	−37.797556	−0.37051	3.27155	−1.20364	−37.745361	−0.36436
				CI						CI			CI
11k	99.0	−37.843780	−0.41241	1.70500	0.36141	0.47079	0.63192	−37.797309	−0.37136	3.27684	−1.20610	−37.744893	−0.36693
	99.5	−37.844069	−0.40643	1.70495	0.36143	0.47529	0.63186	−37.797568	−0.36819	3.27677	−1.20604	−37.745357	−0.36179
	99.7	−37.844179	−0.40455	1.70474	0.36139	0.46821	0.63181	−37.797740	−0.36500	3.27651	−1.20576	−37.745523	−0.35869
	99.8	−37.844255	−0.40344	1.70510	0.36150	0.45312	0.63185	−37.797794	−0.36429	3.27653	−1.20581	−37.745561	−0.35805
	99.9	−37.844291	−0.40282	1.70508	0.36151	0.45521	0.63183	−37.797830	−0.36388	3.27665	−1.20586	−37.745588	−0.35766
	99.95	−37.844301	−0.40274	1.70507	0.36151	0.45549	0.63182	−37.797840	−0.36374	3.27661	−1.20583	−37.745600	−0.35750
12k	99.0	−37.843884	−0.41263	1.70501	0.36141	0.47288	0.63150	−37.797430	−0.37156	3.27675	−1.20574	−37.745020	−0.36712
	99.3							−37.797596	−0.36938	3.27692	−1.20577	−37.745388	−0.36357
	99.5	−37.844173	−0.40664	1.70495	0.36143	0.47731	0.63145	−37.797689	−0.36838	3.27668	−1.20567	−37.745483	−0.36198
	99.7	−37.844284	−0.40476	1.70474	0.36140	0.47023	0.63140	−37.797860	−0.36523	3.27644	−1.20542	−37.745655	−0.35871
	99.8	−37.844346	−0.40392	1.70510	0.36150	0.45486	0.63145	−37.797914	−0.36452	3.27649	−1.20550	−37.745689	−0.35821
	99.9	−37.844396	−0.40303	1.70509	0.36152	0.45670	0.63143	−37.797951	−0.36407	3.27661	−1.20558	−37.745716	−0.35782
	99.95	−37.844406	−0.40295	1.70507	0.36152	0.45698	0.63142	−37.797962	−0.36394	3.27657	−1.20556	−37.745728	−0.35766
13l	99.0	−37.844003	−0.41282	1.70505	0.36137	0.47353	0.63153	−37.797580	−0.37182	3.27690	−1.20549	−37.745181	−0.36736
Final		−37.844525	−0.40314	1.70511	0.36148	0.45699	0.63144	−37.798111	−0.36420	3.27672	−1.20531	−37.745889	−0.35790

angular coefficients in the log-log figure is ∼1. The slope of this correlation is slightly smaller than 1 for the convergence in n and is about 10–20 for the convergence in p, as can be seen from the offsets in the log-log figure. Similar behaviors where found in the open-core CI calculations of S^- [24], Cl, and Cl^- [25]. In general, we can make the following observations [37]: The CSFs that are important for the energy are accordingly important for the $S_{\rm sms}$, and the $S_{\rm sms}$ value is more sensitive to the choice of the CSF space than to the orbital basis set.

The energy, $S_{\rm sms}$, and hyperfine parameters calculated in this work are presented in Table I for neutral carbon and in Table II for C^-. It should be stressed that the differences between the results obtained with $p = 99.9$ and $p = 99.95$ are close to the expected numerical accuracy. We estimate that the dominant error in the neutral carbon calculations is due to the nl truncation of the active set. This is not the case in the C^- calculations for which the p truncation is the most limiting.

From Tables I and II, we observe that the differences between the MR_p-I$\lceil 11k \rceil$ and MR_p-I$\lceil 12k \rceil$ results do not depend strongly on p. In fact, the error made by reporting the impact of the 12th shell on the calculation with $p = 99$ on the results of the largest MR_p-I$\lceil 11k \rceil$ is smaller than $4 \times 10^{-7}\ E_h$ on the energy, smaller than $2 \times 10^{-6} a_0^{-2}$ on $S_{\rm sms}$, and smaller than $9 \times 10^{-5} a_0^{-3}$ on the hyperfine parameters.

Using this observation, we add a correction for the 13th correlation layer and for the $l = 8$ orbitals. First MCHF calculations are performed on the MR-I$\lceil 13k \rceil$ and MR-I$\lceil 12l \rceil$ CSF spaces, fixing all one-electron radial functions at the MR-I$\lceil 12k \rceil$ level and varying only the new orbitals. We use the so-optimized orbitals in MR_{99}-I$\lceil 13l \rceil$ CI calculations, omitting the $13l$ subshell in the active set and using the multireference obtained with the $\lceil 12k \rceil$ active set. The two contributions (higher n and l) are of same order of magnitude, as far as the energy is concerned. Still, the additional correlation layer tends to dominate in C^- while the additional angular flexibility has the largest impact in the neutral carbon calculations.

As mentioned, the convergences in either n or p of a state energy and $S_{\rm sms}$ are monotone and correlated (see, e.g., Fig. 2). This fact could help strongly for extrapolating the energy and $S_{\rm sms}$ value. However, even for a two-electron system, the precise behavior of the energy convergence with the principal quantum number in the high-n limit is unknown [38,39]. Froese-Fischer used the following extrapolation function for

TABLE II. Results of the MCHF and CI calculations performed for the C^- $2p^3\,^4S^o$ and $^2D^o$ terms. The energies E are in units of E_h, the $S_{\rm sms}$ in units of a_0^{-2}, and the hyperfine parameters in units of a_0^{-3}. The final values are the results of the larger $\lceil 12k \rceil$ calculations on which the impact of the 13th shell and $l = 8$ orbitals has been additively transferred.

Model		$1s^22s^22p^3\,^4S^o$			$1s^22s^22p^3\,^2D^o$					
nl	p	E	$S_{\rm sms}$	a_c	E	$S_{\rm sms}$	a_l	$a_{\rm sd}$	a_c	b_q
					MCHF					
HF		−37.708844	−1.60530	0.0	−37.642589	−1.54597	2.35963	0.47193	0.0	0.0
4		−37.862042	−0.56521	0.33257	−37.810185	−0.51517	2.27217	0.50749	0.23109	0.10808
5		−37.876688	−0.56168	0.18050	−37.827492	−0.51410	2.28209	0.54068	0.23971	0.12912
6		−37.884109	−0.54166	0.55357	−37.836040	−0.49077	2.25909	0.52516	0.35738	0.15402
7		−37.887227	−0.54675	0.43564	−37.839993	−0.49006	2.23484	0.52138	0.31616	0.18659
8k		−37.888691	−0.54785	0.41389	−37.841966	−0.49306	2.22493	0.52273	0.30328	0.19303
9k		−37.889449	−0.54912	0.46136	−37.842933	−0.49444	2.21796	0.52136	0.32378	0.19962
10k		−37.889853	−0.54975	0.45976	−37.843464	−0.49534	2.21563	0.51911	0.32252	0.20107
11k		−37.890085	−0.55017	0.45517	−37.843751	−0.49583	2.21476	0.51910	0.32312	0.20291
12k		−37.890213	−0.55042	0.45714	−37.843927	−0.49614	2.21462	0.51922	0.32144	0.20238
					CI					
11k	99.0	−37.890143	−0.54957	0.46140	−37.844634	−0.48786	2.20369	0.51222	0.30714	0.21266
	99.3	−37.890301	−0.54774	0.45872	−37.844971	−0.48375	2.20081	0.51100	0.30452	0.21527
	99.5	−37.890474	−0.54414	0.44761						
	99.7	−37.890640	−0.54204	0.43942						
	99.8	−37.890692	−0.54132	0.43823						
12k	99.0	−37.890271	−0.54982	0.46325	−37.844826	−0.48798	2.20269	0.51165	0.30450	0.21262
	99.3	−37.890440	−0.54797	0.46098	−37.845165	−0.48386	2.19983	0.51040	0.30176	0.21519
	99.5	−37.890603	−0.54438	0.44919						
	99.7	−37.890769	−0.54227	0.44080						
	99.8	−37.890822	−0.54151	0.43945						
13l	99.0	−37.890429	−0.55003	0.46636	−37.845003	−0.48828	2.20286	0.51161	0.30547	0.21300
Final		−37.890980	−0.54172	0.44257	−37.845343	−0.48415	2.20000	0.51036	0.30273	0.21557

studying four electrons systems [40]:

$$\Delta E_n = a_4/(n-\delta n)^4 + a_5/(n-\delta n)^5 + a_6/(n-\delta n)^6, \quad (22)$$

with the a_4, a_5, and a_6 parameters and δn being chosen such that $a_4 < 0$ and $|a_4| \sim |a_5| \sim |a_6|$. Fitting the $n = 10$–12 results of Table I to Eq. (22) for extrapolating to $n \to \infty$, we obtain −37.84465 E_h for the energy of the $C(^3P)$ state. This procedure does not extrapolate to $l \to \infty$. The error on the extrapolation is of the order of 10^{-5} E_h and the truncation in l of about 10^{-4} E_h. We are in fair agreement with the nonrelativistic energy of −37.8450 E_h estimated by Chakravorty *et al.* [41]. To our knowledge, the values of Table I are the best *ab initio* estimated energies, even without the $n = 13$ and $l = 8$ corrections. Finally, let us mention that Sarsa *et al.* [42] calculated the $S_{\rm sms}$ expectation value for the carbon ^3P state using the Monte Carlo (MC) approach with an explicitly correlated wave function and obtained $S_{\rm sms} = -0.38(2)\ a_0^{-2}$. Our final estimated value ($-0.40314\ a_0^{-2}$) falls a bit outside the statistical MC error bars.

F. Breit-Pauli calculations

A first way to include relativistic effects is to use the Breit-Pauli Hamiltonian that includes the $1/c^2$ relativistic correction operators to the nonrelativistic atomic Hamiltonian [27].

Since the radiative transitions we consider are essentially authorized by L and S mixing, we need to have a good description of the term mixing. On the other hand, it is the calculation of the scalar relativistic effects that is needed for estimating the relativistic effects on the electron affinity since the fine structures of the involved species are usually known experimentally. We therefore choose two distinct Breit-Pauli models. The first BPCI CSF lists are used for the term separation and detachment thresholds corrections while the second approach is used for the transition probabilities calculations.

Focusing on the correlation, we merge the MR_{99}-I$\lceil 10k \rceil$ lists of the studied terms for both C^- and C. Then we extend this model by adding the CSFs interacting to first order with the CSFs $2p3p\ LS$, $LS = {}^3D, {}^3S, {}^1P$ for C and the CSFs $2p^2\ 3p\ LS$, $LS = {}^2P^o, {}^2F^o, {}^4D^o, {}^4P^o$ for C^-. For the neutral carbon we test the impact of additional correlation on the relativistic corrections by using the MR_{99}-I$\lceil 11k \rceil$ and $MR_{99.5}$-I$\lceil 11k \rceil$ spaces. We finally diagonalize the Breit-Pauli Hamiltonian in those CSF spaces using the corresponding active sets optimized in the nonrelativistic calculations. The relativistic corrections to the energy are summarized in Table III. We see that the effect of the additional LS mixing on the energy levels is so small that only the corrections on the fine structures are meaningful.

TABLE III. Relativistic corrections (in unit of μE_h) to the total energies evaluated by BPCI calculations (see text).

Model		C $1s^2 2s^2 2p^2$					C$^-$ $1s^2 2s^2 2p^3$		
nl	p	$^3P_0$	$^3P_1$	$^3P_2$	$^1D_2$	$^1S_0$	$^4S^o_{3/2}$	$^2D^o_{3/2}$	$^2D^o_{5/2}$
					Main spectroscopic terms only (see text)				
$10k$	99	−14 437.25	−14 362.42	−14 239.95	−14 288.85	−14 256.62		−14 200.89	−14 192.92
$11k$	99	−14 409.01	−14 334.21	−14 211.76	−14 330.16	−14 296.56			
$11k$	99.5	−14 455.75	−14 380.91	−14 258.35	−14 331.96	−14 299.28			
					With additional spectroscopic terms (see text)				
$10k$	99	−14 437.25	−14 362.63	−14 240.02	−14 288.99	−14 256.62	−14 129.53	−14 201.14	−14 193.15
$11k$	99	−14 409.01	−14 334.42	−14 211.82	−14 330.30	−14 296.56			

For the reasons expressed above, we also perform BPCI calculations that focus on term mixing. For each LSJ and active set $\lceil nl \rceil$ ($nl = 4f - 12k$ for C and $4f - 8k$ for C$^-$), the MR$_{98}$-I list is merged with the MR-I set obtained using the reference containing all allowed LS couplings of the $2s \to 3d$, $2p \to 3p$, and $2s^2 \to 2p^2$ excitations from the main configuration.

G. Relativistic configuration interaction calculations

We use essentially the same method as in Ref. [33]. First, we perform reference MCHF calculations with all single and double configuration excitations (SD) of the ground state in active sets ranging from $\lceil 3d \rceil$ to $\lceil 8k \rceil$. The resulting nonrelativistic radial orbitals $P_{nl}(r)$ are then converted to Dirac spinors using the Pauli approximation

$$P_{n\kappa}(r) = P_{nl}(r) \tag{23}$$

$$Q_{n\kappa}(r) = \frac{\alpha}{2}\left(\frac{d}{dr} + \frac{\kappa}{r}\right) P_{nl}(r) \tag{24}$$

where α is the fine-structure constant and κ is defined

$$\kappa = \begin{cases} -l-1 & \text{when} \quad j = l + 1/2 \\ l & \text{when} \quad j = l - 1/2 \end{cases}. \tag{25}$$

With these spinors, we finally perform the corresponding RCI calculations, using the RCI2 program of the GRASP2K package [28]. The corresponding calculations are labeled "MCHF-RCI." Expansions based on SD excitations of the main configuration are first considered. Larger configuration sets are also explored using the following multireference sets

$$\mathrm{MR(C^-)} = \{1s^2 2s^2 2p^3, 1s^2 2s^1 2p^3 3d^1\}, \tag{26}$$

$$\mathrm{MR(C)} = \{1s^2 2s^2 2p^2, 1s^2 2s^1 2p^2 3d^1, 1s^2 2p^4\}. \tag{27}$$

The relativistic effects are estimated from the differences between the nonrelativistic CI and corresponding RCI results.

Table IV presents the relativistic corrections on the S_{sms} parameter. In the monoconfiguration model, the S_{sms} differences between the Hartree-Fock (HF) and the corresponding HF-RCI values are first reported and compared with the differences obtained in the Dirac-Fock (DF) approach. The multiconfigurational mono- and multireference relativistic corrections deduced from the MCHF-RCI calculations are then presented for increasing orbital active sets. Electron correlation plays an important role in the estimation of these corrections, as could be expected from an operator that measures the correlation between the momenta of the electrons. A good convergence of the monoreference approach with n is achieved but substantial changes are observed between the mono- and multireference results. In Table V, we present the corresponding corrections for $A\frac{I}{\mu_I}$ and B/Q that are both independent of the nuclear spin I and multipole moments (μ_I, Q).

Similarly to the nonrelativistic calculations, we note that for neutral carbon, the impact of the 7$^{\mathrm{th}}$ and 8$^{\mathrm{th}}$ shells is not much affected by the choice of reference. We then estimate the final value as in the nonrelativistic case.

III. RESULTS AND COMPARISON TO EXPERIMENT

A. Hyperfine structures

In this work, we focus on the isotopes 13 and 11 of carbon, respectively, of nucleus spin 1/2 and 3/2. The ^{11}C nucleus decays into ^{11}B by e^+ emission with a half-lifetime of 20.4 minutes. Haberstroh *et al.* [45] and Wolber *et al.* [43] performed experimental studies of the hyperfine structures

TABLE IV. Relativistic corrections to the S_{sms} specific mass shift parameter evaluated by MCHF-RCI calculations. Results are presented in units of $10^{-6}\ a_0^{-2}$.

Model	C $2p^2$					C$^-$ $2p^3$		
	$^3P_0$	$^3P_1$	$^3P_2$	$^1D_2$	$^1S_0$	$^4S^o_{3/2}$	$^2D^o_{3/2}$	$^2D^o_{5/2}$
				Monoconfigurational				
HF-RCI	−47	−47	−47	−49	−53	−58	−61	−61
HF-DF	−876	−560	65	−243	−233	−91	−57	−40
				Multiconfigurational, monoreference				
3	62	190	375	316	343	449	439	442
4	4555	4769	5143	4933	4859	5080	4993	5011
5	3996	4228	4636	4388	4413	4595	4678	4700
6	3837	4067	4473	4259	4376	4230	4131	4154
7	3918	4157	4579	4338	4324	4305	4180	4210
8	3939	4175	4593	4337	4338	4329	4272	4304
				Multiconfigurational, multireference				
3	98	225	412	351	390	441	442	449
4	4750	4967	5349	5128	5134	5201	5106	5128
5	4167	4402	4817	4559	4633	4713	4794	4820
6	3999	4233	4647	4426	4570	4347	4241	4268
7	4081	4323	4752	4506	4509			
Final	4102	4341	4766	4506	4523	4446	4382	4418

TABLE V. Relativistic corrections to $A\frac{I}{\mu_I}$ (kHz per unit of μ_N) and B/Q (kHz/barn) evaluated by MCHF-RCI calculations.

Model	$2p^2\,^3P$				$2p^2\,^1D$		$2p^3\,^4S^o$		$2p^3\,^2D^o$			
($n_{\max}$)	A_1	B_1	A_2	B_2	A_2	B_2	$A_{3/2}$	$B_{3/2}$	$A_{3/2}$	$B_{3/2}$	$A_{5/2}$	$B_{5/2}$
Monoconfigurational												
HF-RCI	93	2	118	90	−141	−82	2	0.1	69	855	−24	0
HF-DF	−158	−10	164	−177	−26	150	−122	−0.2	−464	550	371	0
Multiconfigurational, monoreference												
3	−221	−51	−52	38	−166	−130	−404	−0.4	−62	1317	−113	26
4	−226	−31	157	−111	−23	61	−301	−0.1	−18	1276	50	24
5	−256	−34	152	−121	−13	70	−322	0.0	−16	1280	68	23
6	−254	−35	163	−123	−3	64	−319	0.2	−19	1356	73	27
7	−279	−39	158	−135	6	71	−357	−0.1	−19	1393	77	36
8	−285	−35	160	−146	11	85	−368	−0.1	−16	1392	81	36
Multiconfigurational, multireference												
3	−221	−52	−52	38	−168	−132	−414	−0.4	−66	1267	−117	25
4	−217	−34	166	−106	−24	52	−289	−0.1	−26	1210	52	25
5	−246	−37	162	−115	−14	59	−306	0.0	−25	1218	71	24
6	−242	−38	174	−116	−4	52	−298	0.1	−30	1291	78	28
7	−266	−42	170	−128	6	57						
Final	−272	−38	172	−138	10	71	−347	−0.1	−27	1328	86	38

of the carbon ground state of ^{11}C and ^{13}C, respectively. In the latter article, a magnetic dipole-moment of ^{11}C of $-0.964(1)$ μ_N was deduced from the then-available $\mu(^{13}C)$ value. We update this estimation by using the modern $\mu(^{13}C)$ value [46] combined with the two measured $A(^3P_2)$ constants:

$$\mu(^{11}C) = \left[\frac{A_2(^{11}C)\, I_{11}\, \mu(^{13}C)}{A_2(^{13}C)\, I_{13}}\right]_{\text{expt}} = -0.9642(2)\ \mu_N. \quad (28)$$

The error on this value is now dominated by the accuracy of the $A(^3P_2)$ hyperfine constants measurements.

As mentioned in Sec. II E, it is difficult to have a rigorous estimate of the uncertainty on the hyperfine parameters. We, however, advance a learned guess of their reliability. First, we see in Table I that the integrals a_l, a_{sd}, and b_q of C change less than 0.05% after the addition of the $\lceil 13l \rceil$ correction. The a_c parameter of the ^3P is only slightly more affected (∼0.1%). These effects are representative of the accuracy of our results for neutral carbon. In the case of C^- we face two additional limitations: The structure of the negative ion converges more slowly and we are limited in our expansions. Moreover, only the most troublesome contact term is responsible for the nonrelativistic HFS of $2p^3\,^4S^o$. For these reasons, and comparing the values of Table II with results obtained with the active set $\lceil 10k \rceil$, we must allow for relative uncertainties on the HFS parameters roughly 10 times larger for C^- than for C.

In Table VI, we present the nonrelativistic $A\frac{I}{\mu_I}$ and B/Q results calculated using the final values of a_l,a_{sd},a_c, and b_q of Tables I and II. In the same table, we add the relativistic corrections of Table V to those values. The $A(^3P_1)$ constant is the place of severe compensations between the orbital (a_l) and spin-dipole (a_{sd}) contributions, and the uncertainties on those sum up to an error of the order of 10^2 kHz/μ_N. The other nuclear-parameter-independent hyperfine constants of neutral carbon suffer of a nonrelativistic uncertainty of about 10–10^2 kHz/μ_N. These are larger than the fluctuations observed in Table V. As far as C^- is concerned, on the one hand, the $^4S^o$ hyperfine structure is essentially due to the contact term, itself arising only from correlation effects and, on the other hand, the $^2D^o$ hyperfine constants are small but the achieved

TABLE VI. $A\frac{I}{\mu_I}$ (kHz per unit of μ_N) and B/Q (kHz/barn) theoretical values for carbon ^3P, ^1D and C^- $^4S^o$, $^2D^o$.

State	C $A\frac{I}{\mu_I}$	B/Q	State	C^- $A\frac{I}{\mu_I}$	B/Q
Nonrelativistic					
$2p^2\,^3P_1$	2296	74 184	$2p^3\,^4S^o_{3/2}$	9394	0
$2p^2\,^3P_2$	105 883	−148 367	$2p^3\,^2D^o_{3/2}$	53 836	−35 455
$2p^2\,^1D_2$	156 317	283 206	$2p^3\,^2D^o_{5/2}$	107 317	−50 650
+Relativistic corrections					
$2p^2\,^3P_1$	2024	74 145	$2p^3\,^4S^o_{3/2}$	9048	0
$2p^2\,^3P_2$	106 055	−148 505	$2p^3\,^2D^o_{3/2}$	53 809	−34 128
$2p^2\,^1D_2$	156 327	283 276	$2p^3\,^2D^o_{5/2}$	107 403	−50 613

TABLE VII. Comparison of our calculated hyperfine constants of ^{13}C to other works. The experimental values are adjusted according to our analysis of the off-diagonal JJ' interaction. All values are in MHz.

	^{13}C			^{13}C$^-$		
	$A_1(^3P)$	$A_2(^3P)$	$A_2(^1D)$	$A_{3/2}(^4S^o)$	$A_{3/2}(^2D^o)$	$A_{5/2}(^2D^o)$
Original expt.[a]	2.838(17)	149.055(10)				
This work	2.84	148.99	219.61	12.71	75.59	150.88
Prev. work[b]	2.28	148.1				

[a]Reference [43].
[b]Reference [44].

convergence of the calculations is less good. Therefore the relative nonrelativistic uncertainties on C$^-$ hyperfine structures are larger as they sum up to about 50–100 kHz/μ_N (kHz/barn). We conclude that the reliability of all normalized hyperfine constants is of the order of 10^2 kHz/μ_N (kHz/barn) with the exception of the $B(^4S^o)$ that is certainly negligible.

Our results are compared with observations in Tables VII and VIII for ^{13}C and ^{11}C respectively. We observe a good agreement with experiment, better than expected from the above discussion. This represents a significant improvement compared to the theoretical study of Jönsson *et al.* [44].

The observed hyperfine splittings arise from the diagonal hyperfine interaction, parametrized by the A_J and B_J constants and, to higher order, from the nondiagonal (JJ') interaction of states of same F. If only two levels are involved, one must diagonalize the matrix

$$\begin{bmatrix} 0 & W(JJ';F) \\ W(JJ';F) & \Delta_{JJ'}E(LS\,F) \end{bmatrix}, \tag{29}$$

where $\Delta_{JJ'}E(LS\,F) = E(LSJ'F) - E(LSJF)$ is dominated by the fine-structure splitting and $W(JJ';F)$ is governed by the off-diagonal hyperfine constants (here $A_{J,J-1}$, $B_{J,J-1}$, and $B_{J,J-2}$; see Sec. II B). The off-diagonal electric quadrupole interaction is negligible and, at the nonrelativistic level, we obtain for C(^3P)

$$IA_{1,0}/\mu_I = 50.47\ \text{MHz}/\mu_N, \tag{30}$$
$$IA_{2,1}/\mu_I = 62.71\ \text{MHz}/\mu_N, \tag{31}$$

while for C$^-$($^2D^o$) we have

$$IA_{5/2,3/2}/\mu_I = 34.20\ \text{MHz}/\mu_N. \tag{32}$$

The hyperfine interaction between states belonging to different terms is negligible.

Wolber *et al.* [43] measured two hyperfine splittings in the ^{13}C ^3P_J multiplet, allowing the determination of the A_1 and A_2 diagonal constants but not of the off-diagonal constants so that they had to deduce the contribution of the JJ' interaction theoretically. The level shifts that they obtained from their computations are significantly higher than ours. However, the A_J constants that reproduce the experimental hyperfine splittings when using our results for the JJ' interaction, $A_1 = 2.829(17)$ MHz and $A_2 = 149.052(10)$ MHz, do not differ largely from the experimental constants presented in Table VII.

Haberstroh *et al.* [45] measured three hyperfine splittings for ^{11}C ^3P_J, which is insufficient for determining all four A_J and B_J of this term. Hence, they deduced the value of B_1 from the relation $B_2/B_1 = -2$ which is only valid in the Hartree-Fock model. From Table VI, we see that this formula holds very well at the nonrelativistic level but that, including relativistic corrections, we have

$$B_2/B_1 = -2.0029. \tag{33}$$

The effect of the refined B_2/B_1 ratio and JJ' interactions cancel each other in the estimation of the diagonal hyperfine constants so the resulting A_J constants do no differ significantly from the experimental ones quoted in Table VIII. For the electric quadrupole interaction, the accuracy of our results is such that we can safely update the electric quadrupole moment of the ^{11}C nucleus with the formula

$$Q(^{11}\text{C}) = \frac{[B_2(^{11}\text{C})]_{\text{expt}}}{(B_2/Q)_{\text{theor}}}. \tag{34}$$

TABLE VIII. Comparison of our calculated hyperfine constants of ^{11}C to other works. The experimental values are adjusted according to our analysis of the off-diagonal JJ' interaction and of $B(^3P_1)/B(^3P_2)$. All values are in MHz.

	^{11}C					
	$A_1(^3P)$	$B_1(^3P)$	$A_2(^3P)$	$B_2(^3P)$	$A_2(^1D)$	$B_2(^1D)$
Original expt.[a]	−1.308(24)	2.475(14)	−68.203(7)	−4.949(28)		
This work	−1.30	2.474	−68.17	−4.955	−100.49	9.450
	^{11}C$^-$					
	$A_{3/2}(^4S^o)$	$B_{3/2}(^4S^o)$	$A_{3/2}(^2D^o)$	$B_{3/2}(^2D^o)$	$A_{5/2}(^2D^o)$	$B_{5/2}(^2D^o)$
This work	5.82	≈ 0	34.59	−1.139	69.04	−1.688

[a]Reference [45].

Using the B_2 constant of Haberstroh *et al.* [45], we obtain a value of $+0.03333(19)_{\rm expt}(2)_{\rm theor}$ barns but if we use our theoretical parameters in the analysis of the observations, we obtain

$$Q(^{11}{\rm C}) = +0.03336(19)_{\rm expt}(2)_{\rm theor}\ \text{barns}. \qquad (35)$$

This value is used for estimating the theoretical B_J constants of this work presented in Table VIII. The difference between theory and experiment for the B_2 constant follows directly from the fact that (35) includes the refinements of the theoretical parameters needed in the analysis of the observed hyperfine splittings.

Let us mention the previous calculations of the b_q parameter (we get $b_q = 0.6314\ a_0^{-3}$): $b_q = 0.6325\ a_0^{-3}$ [47] and $b_q = 0.6319\ a_0^{-3}$ [31]. Using the experimental constant B_2 quoted in Table VIII, Sundholm and Olsen [47] proposed $Q(^{11}{\rm C}) = +0.03327(24)$ barns which would only tenuously agree with our estimation if the $[B_2(^{11}{\rm C})]_{\rm expt}$ value was to be improved.

In the case of C^-, the small $^2D^o$ fine structure (1.75 cm^{-1}, see below), leads to JJ'-interaction shifts on the energy levels that are roughly 10 times larger than in the neutral atom ground term, i.e., of the order of 0.1 MHz.

B. Energy differences

Table IX presents several calculated energy separations and compares them to other works. Our C^- term splitting is in very good agreement with experiment but, as will be seen below, this is partially accidental.

Our results on the neutral atom ground configuration level spacings are systematically better than the ones of Froese-Fischer and Tachiev [48]. It indicates that, in this context, our relativistic corrections are reliable. For the ^3P fine structure, we obtain as accurate results as recent fully relativistic calculations [49].

Our systematic procedure is not particularly efficient for predicting the negative ion binding energy. In particular, for the $^4S^o$ detachment threshold, the coupled-cluster approaches are much more impressive [15,16]. The recent value of Klopper *et al.* [16] indeed achieves a submillielectron-volt ($<8\ \text{cm}^{-1}$) agreement with the experimental electron affinities for all first- and second-period atoms (H-Ne). A similar accuracy had already been achieved more than 10 years before by de Oliveira *et al.* [15] for the second and third period p-block atoms.

By trying various extrapolation schemes on our C^- calculations, we explain up to $\sim 20\ \text{cm}^{-1}$ of the difference between our calculation of the $^4S^o$ binding energy and the experimental value (about 5 cm^{-1} for each n and l extrapolations and about another 10 cm^{-1} for the extrapolation to a complete active set). Turning to the relativistic effects calculations, we see that the scalar contributions calculated with the CC methods give $-21.54\ \text{cm}^{-1}$ [16] and $-22.83\ \text{cm}^{-1}$ [15] while we obtain $-37.95\ \text{cm}^{-1}$. The extrapolation being reliable to about a couple of tenths of percentage points and since the additional expected contributions are of the order of the cm^{-1}, we conclude that our BPCI relativistic corrections are still unbalanced. The problem of our relativistic corrections on the detachment thresholds is confirmed by the fact that, looking to Table III, they are not well converged.

Aside from a possible unbalance in the relativistic effects estimation, our error is roughly proportional to the correlation contribution. We see that the differences between the HF and experimental energy separations (see Table IX) are reproduced to ~0.1–0.7%, which is about the percentage of the $C(^3P)$ correlation energy we get. It means that p and n are good indicators of the percentage of the correlation effects included in a model. However, the uncertainty on our relativistic corrections and on the $^2D^o$ missing correlation is too large for an extrapolation based on this observation to be useful, e.g., for improving the experimental determination of the position of the $^2D^o_J$ levels. Indeed, a 0.5% uncertainty on our calculated correlation energies, which is no overestimation, reflects in corrections ranging from $\sim 60\ \text{cm}^{-1}$ in the case of the largest HF-experiment discrepancy, to about 7.5 cm^{-1} for the $^2D^o$-^1S threshold, i.e., of the same order of magnitude than the experimental uncertainty.

We would like to stress another advantage of using the number of correlation layers n and p as parameters for preserving the balance between systems having different numbers of electrons. Observing that our models converge toward the exact solution of the Schrödinger equation, a larger number of electrons demands larger active sets, and that for a given orbital set, p is roughly proportional to the amount of correlation in the model, we affirm that the results obtained with increasing n and p will most often underestimate the photodetachment thresholds. In other words, the detachment thresholds are valuable references for estimating the accuracy of the calculations since their behavior is monotone (as the level energies themselves).

C. Mass isotope shifts

Table X reports the results for the $(A' = 13, A = 12)$ IS on various energy differences and compares them to previous works.

We have seen that the $S_{\rm sms}$ parameter is strongly correlated to the energy, with negative and positive angular coefficients with respect to p and n, respectively. The nonmonotonous behavior of the SMS forbids us to generally conclude that any calculation similar to ours will result in upper or lower bounds to the differences in mass polarization expectation values. In our particular case, however, Tables I and II and Fig. 2 show that the convergence in n is better achieved than in p (truncated to 99.8% or 99.3%). Therefore, we likely overestimate $S_{\rm sms}$. Since we have globally $\Delta S_{\rm sms} > \Delta E$, the estimations of the IS on the detachment thresholds presented below, in particular on the ^eA, are probably overly negative. Furthermore, we estimate that our nonrelativistic values of IS are reliable to about 0.2 m^{-1} if the $C^-(^2D^o)$ is involved and of the order of 10^{-2} m^{-1} if not. Hence we cannot explain the disagreement between the isotope shift on the ^eA of Klopper *et al.* [16] and ours. This is not an isolated discrepancy since we can extract from their results an (18–16) IS on the ^eA of oxygen of -11.7 m^{-1} which is in disagreement with the experimental value of $-7.4(18)$ m^{-1} [57]. Godefroid and Froese-Fischer [23] obtained an IS of $-5.73\ \text{m}^{-1}$ with a MCHF model, which is inside the experimental error bars (see also Ref. [37]). The MCHF approach has also proven its usefulness for the calculation of IS on the ^eA of heavier systems [24,25].

TABLE IX. Comparison of the theoretical and experimental energy level separations. The MCHF – CI calculations of the energy differences involving C^- $^4S^o$ and $^2D^o$ are obtained with $p = 99.8\%$ and 99.3%, respectively, while we take $p = 99.95\%$ for neutral carbon transitions energies. Relativistic corrections (+rel) are estimated from Table III and the $+\lceil 13l \rceil$ column corresponds to the final results of Tables I and II. All values are given in cm^{-1}.

	This work						
State	HF	MCHF – CI	+rel	$+\lceil 13l \rceil$	Expt.	Prev. theor.	
$C^-(^4S^o_{3/2})$	0.0	0.0	0.0	0.0	0.0		
$C^-(^2D^o_{3/2})$	14 541.11	9 936.73	9 921.01	9 916.63	9 913.5(82)[a]		
$C^-(^2D^o_{5/2})$			9 922.76	9 918.39			
$C(^3P_0)$	0.0	0.0	0.0	0.0	0.0	0.0	
$C(^3P_1)$	0.0	0.0	16.39	16.39	16.42[b]	16.33[c]	16.4[d]
$C(^3P_2)$	0.0	0.0	43.31	43.31	43.41[b]	43.03[c]	43.3[d]
$C(^1D_2)$	12 573.20	10 193.42	10 220.55	10 213.76	10 192.63[e]	10 268.23[c]	
$C(^1S_0)$	30 508.75	21 657.45	21 691.79	21 682.40	21 648.01[e]	21 818.60[c]	
C^--C				Detachment thresholds			
$^4S^o_{3/2}$-$^3P_0$	4 438.80	10 200.50	10 132.96	10 141.49	10 179.68(16)[f]	10 184.61[g]	10 185.8[h]
$^4S^o_{3/2}$-$^1D_0$	17 012.00	20 391.04	20 356.04	20 357.77	20 372.31(16)[f]		
$^4S^o_{3/2}$-$^1S_0$	34 947.55	31 853.18	31 825.28	31 824.42	31 827.69(16)[f]		
$^2D^o_{3/2}$-$^3P_0$	−10 102.31	240.39	194.77	207.67	266.2(81)[a]	436[i]	
$^2D^o_{3/2}$-$^1D_2$	2 470.89	10 440.27	10 420.99	10 427.10	10 458.8(81)[a]		
$^2D^o_{3/2}$-$^1S_0$	20 406.44	21 898.72	21 886.54	21 890.05	21 914.2(81)[a]		

[a]Reference [14].
[b]Reference [50].
[c]Reference [48].
[d]Reference [49].
[e]Reference [51].
[f]Reference [13].
[g]Reference [16].
[h]Reference [15].
[i]Reference [8].

With regard to the difficulty to calculate the mass shifts, the discrepancy between the different calculations of the IS on the neutral atom term separation, of the order of 0.1 m^{-1}, is understandable. From the comparison of our results and the ones of Kozlov *et al.* [49], it is difficult to estimate an order of magnitude for the contribution of the relativistic effects.

The neutral ^3P fine structure has been much more studied. It is known that the relativistic corrections to the mass shift operator are crucial when studying the isotope shift on the fine structure [58–61]. Veseth [53] and more recently Kozlov *et al.* [49] performed calculations of the relativistic mass shifts in the ^3P multiplet of carbon, the first by treating perturbatively the fine-structure and nucleus-mass-dependent Hamiltonians up to the third order, the second by using an all-electron CI method on the Dirac-Breit Hamiltonian and calculating the expectation value of the relativistic MS operator valid to the second order in αZ. We easily estimate the relativistic corrections to the specific mass shift operator for the transition $^3P_1$-$^3P_2$ by comparing the equation (8) of Veseth to the Breit-Pauli fine-structure operator.[2] We obtain a correction of $+0.0375$ m^{-1} for the $^{13-12}$IS($^3P_1$-$^3P_2$) which, combined with our result of Table X, gives a total shift of $+0.014$ m^{-1}. This value is in good agreement with the observation and with Veseth's results. However, neither this observation nor the stability of the corrections of Table IV demonstrates that the scalar relativistic effects on the IS are reliable.

D. Transition probabilities

We study the $M1$ and $E2$ transition probabilities between the LSJ levels of the ground configurations of C and C^-. With the exception of $^1D_2$-$^1S_0$ and the transitions between states of a same multiplet, the calculated Einstein coefficients are only nonzero thanks to the LS relativistic mixing. The $M1$ channel of the $^4S^o_{3/2}$-$^2D^o_{5/2}$ transition is itself only opened by LS mixing of correlation CSFs. The nonrelativistic magnetic dipole and electric quadrupole transition amplitudes are computed using the BPCI wave functions based on the MR_{98}-I model described in the end of Sec. II F. For the calculation of the Einstein A transition rates between states that are developed in nonorthogonal orbital sets, we use the BIOTR program that is part of the the ATSP2K package [26]. Although the velocity form of the $E2$ transition probabilities is produced by this program, we do not report the corresponding values since the

[2]From Ref. [53], we find that the relativistic corrections to the IS on the fine structure can be estimated using the Table VI of Veseth's paper as $2/3[(8d) + (8e)] + (8f)$.

TABLE X. Comparison of our isotope shifts ($A' = 13, A = 12$), in m^{-1}, on various positive energy separations. The MCHF – CI calculations of the energy differences involving C^- $^4S^o$ and $^2D^o$ are obtained with $p = 99.8\%$ and 99.3%, respectively, while $p = 99.95\%$ for neutral carbon transitions. Relativistic corrections (+rel) are estimated from Table IV and the $+\lceil 13l \rceil$ column corresponds to the final results of Tables I and II.

	SMS			NMS	IS		
Trans.	MCHF – CI	+rel	$+\lceil 13l \rceil$	Expt.	This work	Other theor.	Expt.
			IS on the C^- terms separations				
$^4S^o_{3/2}$-$^2D^o_{3/2}$	−4.965	−4.960	−4.953	3.500	−1.454		
			IS on the C^- detachment thresholds				
$^4S^o_{3/2}$-$^3P_0$	−10.656	−10.629	−10.630	3.592	−7.038	−8.7[a]	
$^2D^o_{3/2}$-$^1D_2$	−8.865	−8.875	−8.878	3.690	−5.185		
			IS on the C terms separations				
$^3P_0$-$^1D_2$	−3.021	−3.052	−3.047	3.597	+0.550	+0.505[b]	
$^3P_0$-$^1S_0$	−3.507	−3.540	−3.536	7.640	+4.103	+4.672[b]	
						+4.374[c]	
			IS on the C(^3P) fine structure				
$^3P_1$-$^3P_2$	0	−0.033	−0.033	0.010	−0.023	+0.020[b]	+0.0137(10)[d]
					+0.014[e]	+0.015[f]	+0.0180(43)[g]
$^3P_0$-$^3P_1$	0	−0.019	−0.019	0.006	−0.013	+0.009[b]	+0.0077(7)[h]
						+0.010[f]	+0.0057(83)

[a]Nonrelativistic coupled-cluster calculations [16].
[b]Calculations using the Dirac-Breit Hamiltonian and the relativistic mass shift operator [49]. Note that they used a different sign convention than ours (Kozlov, private communication).
[c]MCHF-CI calculations [52]. SMS = -3.266 m^{-1}.
[d]Reference [50].
[e]Our results combined with the relativistic corrections of Veseth [53] (see text).
[f]MBPT calculations of the relativistically corrected mass shift operator [53]. Note that those values are quoted with the wrong sign in Ref. [54], as pointed out in Ref. [55].
[g]Reference [54].
[h]Measurements of Ref. [56] and hyperfine splittings of Ref. [43].

length form is the only one strictly reliable for weak amplitudes estimated in the Breit-Pauli scheme.

The results of our calculations on the neutral atom are summarized in Table XI. The convergence of the A coefficients with the active set is well achieved and the comparison with the results of Froese-Fischer [62] is favorable. Still, we can point out that, for the weak $E2$ transition rates of interterm transitions ($^3P_0$-$^1D_2$ and $^3P_1$-$^1D_2$), the relative

TABLE XI. Einstein A coefficients, in s^{-1}, for the $2p^2$ intraconfiguration $M1$ and $E2$ transitions of carbon calculated using the BPCI wave functions based on the MR_{98}-I models for the active space $\lceil 10k \rceil$ and $\lceil 12k \rceil$, compared with the calculations of Ref. [62]. Transitions vacuum wavelengths (λ) are reported in angstroms. The notation ($\pm n$) represents $\times 10^{\pm n}$.

		This work						
		$n = 10$		$n = 12$		Froese-Fischer [62]		NIST [63]
States	Type	λ	A_{ki}	λ	A_{ki}	λ	A_{ki}	λ
$^3P_0$-$^3P_1$	$M1$	6072(+3)	8.033(−8)	6070(+3)	8.041(−8)	6052(+3)	8.114(−8)	6097(+3)
$^3P_1$-$^3P_2$	$M1$	3703(+3)	2.656(−7)	3701(+3)	2.660(−7)	3700(+3)	2.662(−7)	3704(+3)
	$E2$		3.529(−15)		3.536(−15)		3.633(−15)	
$^3P_0$-$^3P_2$	$E2$	2300(+3)	1.696(−14)	2299(+3)	1.700(−14)	2296(+3)	1.754(−14)	2304(+3)
$^3P_2$-$^1D_2$	$M1$	9805	2.370(−4)	9814	2.358(−4)	9735	2.245(−4)	9853
	$E2$		1.210(−6)		1.209(−6)		1.140(−6)	
$^3P_1$-$^1D_2$	$M1$	9779	7.513(−5)	9788	7.504(−5)	9710	7.544(−5)	9827
	$E2$		1.050(−7)		1.037(−7)		1.576(−7)	
$^3P_0$-$^1D_2$	$E2$	9763	7.789(−8)	9772	7.836(−8)	9694	6.242(−8)	9811
$^3P_2$-$^1S_0$	$E2$	4604	2.138(−5)	4606	2.130(−5)	4587	2.250(−5)	4629
$^3P_1$-$^1S_0$	$M1$	4598	2.368(−3)	4600	2.367(−3)	4581	2.381(−3)	4623
$^1D_2$-$^1S_0$	$E2$	8679	6.148(−1)	8681	6.135(−1)			8730

TABLE XII. Einstein A coefficients, in s^{-1}, for the intraconfiguration $M1$ and $E2$ transitions of all C^- bound states, calculated using the BPCI wave functions based on the MR_{98}-I models for the active space $\lceil 4f \rceil$ to $\lceil 8k \rceil$. We compare these results with the corresponding nitrogen and nitrogen-like oxygen A coefficients. Transitions vacuum wavelengths (λ) are reported in angstroms. The final set is obtained by renormalizing the transition probabilities $\lceil 8k \rceil$ with the experimental ($^4S^o$-$^2D^o$) and calculated ($^2D^o_{3/2-5/2}$) energy differences. The notation ($\pm n$) represents $\times 10^{\pm n}$.

	$^4S^o_{3/2}$-$^2D^o_{3/2}$			$^4S^o_{3/2}$-$^2D^o_{5/2}$			$^2D^o_{3/2}$-$^2D^o_{5/2}$		
	λ	$M1$	$E2$	λ	$M1$	$E2$	λ	$M1$	$E2$
					C^- ($Z = 6$)				
$n = 4$	8813	1.177(−6)	7.628(−7)	8815	4.823(−8)	1.118(−6)	−5716(+4)	8.664(−11)	3.108(−22)
$n = 5$	9356	1.130(−6)	8.915(−7)	9357	4.197(−8)	1.297(−6)	−1245(+5)	8.415(−12)	3.912(−23)
$n = 6$	9590	1.126(−6)	1.019(−6)	9590	3.999(−8)	1.470(−6)	−6509(+5)	5.893(−14)	2.141(−26)
$n = 7$	9801	1.123(−6)	1.125(−6)	9800	3.802(−8)	1.605(−6)	1519(+5)	3.092(−12)	4.209(−23)
$n = 8$	9930	1.080(−6)	1.192(−6)	9929	3.663(−8)	1.688(−6)	9908(+4)	1.109(−11)	5.206(−22)
Final		1.030(−6)	1.102(−6)		3.493(−8)	1.559(−6)		5.771(−11)	
					N ($Z = 7$)				
FFT[a]	5199	1.595(−5)	4.341(−6)	5202	9.710(−7)	6.595(−6)	−1148(+4)	1.071(−8)	
BZ nr[b]		1.716(−5)	3.822(−6)		1.046(−6)	5.880(−6)	−1085(+4)	1.239(−8)	
BZ[b]		1.896(−5)			2.445(−7)			1.239(−8)	
					O^+ (Z = 8)				
FFT[b]	3727	1.414(−4)	2.209(−5)	3730	7.416(−6)	3.382(−5)	−5071(+3)	1.241(−7)	
Z87 nr[c]		1.45(−4)	2.13(−5)		7.58(−6)	3.30(−5)	−5119(+3)	1.30(−7)	
Z87[c]		1.58(−4)			2.00(−6)			1.30(−7)	

[a]Reference [48].

[b]Reference [67]; nr denotes that the nonrelativistic form of the $M1$ operator is used.

[c]Reference [68]; nr denotes that the nonrelativistic form of the $M1$ operator is used.

change between the results of Froese-Fischer and ours is quite large.

The results for the C^- are displayed in Table XII. There is no other value available in the literature. To fill this gap, we compare our transition probabilities with others for the first elements of its isoelectronic sequence, i.e., N I and O II. *A priori*, the omission of the relativistic corrections to the $M1$ transition operator [4,64] could be a serious limitation of our calculations. Indeed, Eissner and Zeippen [65] showed that for transitions between terms of the $2p^3$ configuration, in particular, the relativistic corrections are of the same order of magnitude as the usual nonrelativistic amplitude (see N I and O II data of Table XII).

However, as can be seen from Table XII and in Ref. [66], if the $M1$ channel becomes rapidly dominant with increasing Z along the nitrogen-like sequence, the $E2$ channel remains, for low Z, of the same order of magnitude as the $M1$ channel. Furthermore, in the case of the C^- system, the relativistic mixing of the $^2D^o_{3/2}$ and $^4S^o_{3/2}$ is even further suppressed by the diffuse nature of the $^2D^o$ state. The $M1$ channel is then only a small correction to the total A in the C^- ($^4S^o_{3/2}$-$^2D^o_{5/2}$) transition, being of the same order of magnitude as the uncertainty with respect to the convergence with the active set ($\lceil 8k \rceil$–$\lceil 7i \rceil$).

The inversion of the fine-structure splitting of the $^2D^o$ term in C^- with increasing active set reflects the difficulty to calculate this quantity for half-filled shell systems, particularly in highly correlated systems. From this regard, it is also interesting to note that this fine structure is "normal," i.e., not inverted as in the heavier isoelectronic systems. In other words, it tends to behave like a less-than-half-filled-shell system.

The experimental ($^4S^o_{3/2}$-$^2D^o_J$) transition is at 10087(9) Å, and the $^2D^o$ calculated fine structure that we recommend (see Table IX) is +5703 10^4 Å. Table XII presents the final A coefficients calculated with the $\lceil 8k \rceil$ active set and renormalized by the experimental ($^4S^o$-$^2D^o_J$) energy separation, and our theoretical value for the $^2D^o$ fine structure (see Table IX).

IV. CONCLUSION

We performed large-scale MCHF-CI calculations of the energy levels belonging to the lowest configuration of neutral carbon and all bound states of C^-, including the fine structures, hyperfine structures, and isotope shifts. In addition, we calculated all $M1$ and $E2$ transition rates between the studied LSJ states.

The overall precision of the nonrelativistic expectation values is estimated to be about 0.3–0.8%. However, this imprecision on the total energy and $S_{\rm sms}$ leads to a larger uncertainty on the differential effects. To our knowledge, the obtained nonrelativistic energies are the most accurate *ab initio* values to date. We obtained an extrapolated energy for the C(^3P) state of −37.84465 E_h, in good agreement with the semiempirical "exact" value of −37.8450 E_h [41].

We conducted a careful study of the relativistic corrections deduced from the comparison of relativistic CI calculations with the corresponding nonrelativistic calculations. Even if the so-deduced corrections do permit a relevant theory versus experiment comparison and that the correlation effects still dominate our uncertainties in many cases, an estimation of the relativistic effects on a firmer basis should be performed in

more accurate studies. We also note that the C^- negative ion is very little affected by relativity.

We check the experimental hyperfine constants of the neutral carbon by replacing the theoretical parameters used in the original papers [43,45] by our values. The resulting hyperfine constants and ^{11}C nuclear magnetic moments are in good agreement with previous experimental and theoretical studies.

As far as the transitions probabilities calculations are concerned, we find a good agreement of our neutral carbon A coefficients with the ones of the literature. For the C^- intraconfiguration transitions, we expect the relativistic corrections to the $M1$ operator to be less important than in higher Z isoelectronic systems. Once more, the missing correlation effects are equally limiting.

We find that the parametrization of the model in terms of the number of correlation layers ($\sim n$) and percentage of the wave function accounted by the MR in subsequent CI calculations ($=p$) provides useful tools for including a fixed percentage of the total correlation effects. It allows us to establish lower bounds on detachment thresholds and, for calculations that are sufficiently converged with respect to n, upper bounds on ΔS_{sms} (lower bound on S_{sms}).

Note added in proof. Seth *et al.* [69], recently reported the total energy and S_{sms} values computed with the Quantum Monte Carlo method, in agreement with our results. The uncertainty they obtained on their *ab initio* energy is similar to ours while it is significantly larger for the S_{sms}.

ACKNOWLEDGMENTS

T.C. is grateful to the "Fonds pour la formation à la Recherche dans l'Industrie et dans l'Agriculture" of Belgium for a Ph.D. grant (*Boursier F.R.S.-FNRS*). M.R.G. and T.C. thank the *Communauté française of Belgium* (*Action de Recherche Concertée*) for financial support. M.R.G. also acknowledges the Belgian National Fund for Scientific Research (FRFC/IISN Convention). Finally, the authors thank Nathalie Vaeck and Per Jönsson for fruitful discussions.

[1] D. J. Pegg, Rep. Prog. Phys. **67**, 857 (2004).
[2] T. Andersen, Phys. Rep. **394**, 157 (2004).
[3] J. L. Krause, J. D. Morgan III, and R. S. Berry, Phys. Rev. A **35**, 3189 (1987).
[4] M. Nemouchi and M. R. Godefroid, J. Phys. B **42**, 175002 (2009).
[5] B. D. Sharpee, T. G. Slanger, P. C. Cosby, and D. L. Huestis, Geophys. Res. Lett. **32**, 12106 (2005).
[6] B. D. Sharpee, E. R. O'Neill, and T. G. Slanger, J. Geophys. Res. [Space Phys.] **113**, 12301 (2008).
[7] A. Le Padellec, J. Liévin, E. M. Staicu-Casagrande, T. Nzeyimana, E. A. Naji, and X. Urbain, Phys. Rev. A **78**, 062705 (2008).
[8] H.-L. Zhou, S. T. Manson, A. Hibbert, L. Vo Ky, and N. Feautrier, Phys. Rev. A **72**, 032723 (2005).
[9] W. D. Brandon, D. H. Lee, D. Hanstorp, and D. J. Pegg, J. Phys. B **31**, 751 (1998).
[10] G. Y. Kashenock and V. K. Ivanov, J. Phys. B **39**, 1379 (2006).
[11] C. W. Walter, N. D. Gibson, R. C. Bilodeau, N. Berrah, J. D. Bozek, G. D. Ackerman, and A. Aguilar, Phys. Rev. A **73**, 062702 (2006).
[12] P. Andersson, J. Sandström, D. Hanstorp, N. D. Gibson, K. Wendt, D. J. Pegg, and R. D. Thomas, Nucl. Instrum. Methods Phys. Res., Sect. B **266**, 3667 (2008).
[13] M. Scheer, R. C. Bilodeau, C. A. Brodie, and H. K. Haugen, Phys. Rev. A **58**, 2844 (1998).
[14] D. Feldmann, Chem. Phys. Lett. **47**, 338 (1977).
[15] G. de Oliveira, J. M. L. Martin, F. de Proft, and P. Geerlings, Phys. Rev. A **60**, 1034 (1999).
[16] W. Klopper, R. A. Bachorz, D. P. Tew, and C. Hättig, Phys. Rev. A **81**, 022503 (2010).
[17] D. M. Cleland, G. H. Booth, and A. Alavi, J. Chem. Phys. **134**, 024112 (2011).
[18] T. Takao, S. Jinno, K. Hanada, M. Goto, K. Oshikiri, K. Okuno, H. Tanuma, T. Azuma, and H. Shiromaru, J. Phys.: Conf. Ser. **88**, 012044 (2007).
[19] P. Thaddeus, C. A. Gottlieb, H. Gupta, S. Brünken, M. C. McCarthy, M. Agúndez, M. Guélin, and J. Cernicharo, Astrophys. J. **677**, 1132 (2008).
[20] E. A. Hylleraas, Z. Phys. A **54**, 347 (1929).
[21] J. Komasa, W. Cencek, and J. Rychlewski, Phys. Rev. A **52**, 4500 (1995).
[22] M. Stanke, J. Komasa, S. Bubin, and L. Adamowicz, Phys. Rev. A **80**, 022514 (2009).
[23] M. R. Godefroid and C. Froese Fischer, Phys. Rev. A **60**, R2640 (1999).
[24] T. Carette, C. Drag, O. Scharf, C. Blondel, C. Delsart, C. Froese Fischer, and M. R. Godefroid, Phys. Rev. A **81**, 042522 (2010).
[25] T. Carette and M. Godefroid, submitted to J. Phys. B: At. Mol. Opt. Phys. (2011).
[26] C. Froese Fischer, G. Tachiev, G. Gaigalas, and M. R. Godefroid, Comput. Phys. Commun. **176**, 559 (2007).
[27] C. Froese Fischer, T. Brage, and P. Jönsson, *Computational Atomic Structure: An MCHF Approach*, 1st ed. (Taylor & Francis, London, 1997).
[28] P. Jönsson, X. He, C. Froese Fischer, and I. P. Grant, Comput. Phys. Commun. **177**, 597 (2007).
[29] I. Lindgren and A. Rosén, Case Stud. Atom. Phys. **4**, 93 (1974).
[30] A. Hibbert, Comput. Phys. Commun. **9**, 141 (1975).
[31] P. Jönsson, C.-G. Wahlström, and C. Froese Fischer, Comput. Phys. Commun. **74**, 399 (1993).
[32] A. Hibbert, Rep. Prog. Phys. **38**, 1217 (1975).
[33] P. Jönsson, T. Carette, M. Nemouchi, and M. Godefroid, J. Phys. B **43**, 115006 (2010).
[34] W. H. King, *Isotopic Shift in Atomic Spectra* (Plenum, New York, 1984).
[35] M. Godefroid, C. Froese Fischer, and P. Jönsson, J. Phys. B **34**, 1079 (2001).
[36] R. D. Cowan, *The Theory of Atomic Structure and Spectra*, Los Alamos Series in Basic and Applied Series (University of California Press, Berkeley, 1981).
[37] T. Carette, Ph.D. thesis, Université Libre de Bruxelles (2010) [http://theses.ulb.ac.be/ETD-db/collection/available/ULBetd-12132010-195442/].

[38] W. Kutzelnigg, Phys. Chem. Chem. Phys. **10**, 3460 (2008).
[39] T. Helgaker, W. Klopper, and D. P. Tew, Mol. Phys. **106**, 2107 (2008).
[40] C. Froese Fischer, J. Phys. B **26**, 855 (1993).
[41] S. J. Chakravorty, S. R. Gwaltney, E. R. Davidson, F. A. Parpia, and C. Froese Fischer, Phys. Rev. A **47**, 3649 (1993).
[42] A. Sarsa, F. J. Galvez, and E. Buendia, J. Chem. Phys. **110**, 5721 (1999).
[43] G. Wolber, H. Figger, R. A. Haberstroh, and S. Penselin, Z. Phys. A **236**, 337 (1970).
[44] P. Jönsson, C. Froese Fischer, and M. R. Godefroid, J. Phys. B **29**, 2393 (1996).
[45] R. A. Haberstroh, W. J. Kossler, O. Ames, and D. R. Hamilton, Phys. Rev. **136**, B932 (1964).
[46] N. J. Stone, At. Data Nucl. Data Tables **90**, 75 (2005).
[47] D. Sundholm and J. Olsen, J. Chem. Phys. **96**, 627 (1992).
[48] C. Froese Fischer and G. Tachiev, At. Data Nucl. Data Tables **87**, 1 (2004).
[49] M. G. Kozlov, I. I. Tupitsyn, and D. Reimers, Phys. Rev. A **79**, 022117 (2009).
[50] H. Klein, F. Lewen, R. Schieder, J. Stutzki, and G. Winnewisser, Astrophys. J. Lett. **494**, L125 (1998).
[51] C. E. Moore, in *CRC Handbook of Chemistry and Physics*, 76th ed., edited by J. W. Gallagher (CRC Press, Boca Raton, FL, 1993), p. 336.
[52] J. Carlsson, P. Jönsson, M. R. Godefroid, and C. Froese Fischer, J. Phys. B **28**, 3729 (1995).
[53] L. Veseth, Phys. Rev. A **32**, 1328 (1985).
[54] A. L. Cooksy, R. J. Saykally, J. M. Brown, and K. M. Evenson, Astrophys. J. **309**, 828 (1986).
[55] L. Veseth, Phys. Rev. A **35**, 1931 (1987).
[56] S. Yamamoto and S. Saito, Astrophys. J. Lett. **370**, L103 (1991).
[57] C. Blondel, C. Delsart, C. Valli, S. Yiou, M. R. Godefroid, and S. Van Eck, Phys. Rev. A **64**, 052504 (2001).
[58] A. P. Stone, Proc. Phys. Soc. **77**, 786 (1961).
[59] A. P. Stone, Proc. Phys. Soc. **81**, 868 (1963).
[60] C. W. P. Palmer, J. Phys. B **20**, 5987 (1987).
[61] V. M. Shabaev, Phys. Rev. A **57**, 59 (1998).
[62] C. Froese Fischer, J. Phys. B **39**, 2159 (2006).
[63] NIST, "NIST: Atomic Spectra Database," 2010 [http://physics.nist.gov/asd].
[64] G. W. F. Drake, Phys. Rev. A **3**, 908 (1971).
[65] W. Eissner and C. J. Zeippen, J. Phys. B **14**, 2125 (1981).
[66] S. R. Becker, K. Butler, and C. J. Zeippen, Astron. Astrophys. **221**, 375 (1989).
[67] K. Butler and C. J. Zeippen, Astron. Astrophys. **141**, 274 (1984).
[68] C. J. Zeippen, Astron. Astrophys. **173**, 410 (1987).
[69] P. Seth, P. López Rios, and R. J. Needs, J. Chem. Phys. **134**, 084105 (2011).